# Tandem Electron Beam Welding (Report III) †
# – Analysis of Front Wall of Beam Hole by Beam Hole X-ray Observation Method –

Yoshiaki ARATA *, Nobuyuki ABE ** and Susumu YAMAMOTO ***

**Abstract**

*X-ray images emitted from the beam hole have been observed by a pin-hole camera method. The behaviour of the front wall of the beam hole during electron beam welding has been analysed by a high speed movie and a streak photograph. In case of single electron beam welding, the scraping process of the front wall, the formation process of spiking and the suppression mechanism of welding defects by the beam oscillation method have been revealed. It is found that the front wall of the beam hole is not always scraped uniformly but it is scraped by the locally melted region on the front wall. The suppression mechanism of defects by the Tandem Electron Beam Welding Method has been also analysed. It is compared with that of the beam oscillation method in ordinary single electron beam welding. It is suggested that the Tandem Electron Beam Welding Method is much more effective.*

KEY WORDS: (Electron Beam Welding) (X-ray Analysis) (Beam Hole) (Mechanism) (Defects)

## 1. Introduction:

The electron beam welding can utilize an extremely higher power density beam than ordinary welding method. Therefore, it can be applied to a high speed welding of thin plates or a deep penetration welding of thick plates which can not be realized by ordinary methods. However, it is known that special defects such as humping in a high speed welding, spiking and porosity in a deep penetration welding are brought about. It is difficult to suppress these defects by using an ordinary single electron beam welding without disadvantages in welding speed and penetration depth.

In order to overcome these difficulties, the authors have proposed the Tandem Electron Beam Welding Method, which uses two electron beams at a time. This method was applied to a high speed welding with suppressing humping successfully. It has been found that the suppression of humping is caused by the control of the molten metal flow by the second electron beam[1]. This method was also applied to a deep penetration welding with suppressing spiking successfully without disadvantage in penetration depth[2].

In this report, in order to reveal the formation process of spiking in ordinary single electron beam welding and the suppression mechanism of spiking in the Tandem Electron Beam Welding Method, the image of so-called beam hole X-rays emitted from the region where the electron beam interacts with the metal is observed. The behaviour of the X-ray image in a beam oscillation method is also analysed, and then it is compared with that of the Tandem Electron Beam Welding.

## 2. Beam Hole X-ray Observation Method

### 2-1 Observation of beam hole during welding

On the electron beam welding, some experiments have been performed where the shape of the beam hole was observed during welding. For example, Tong and Giedt took transmission X-ray photographs of the beam hole during the electron beam welding by a flush X-ray source with finding that the shape of the beam hole changes with time[3]. Bryant took a series of photographs of the shapes of the beam hole under the welding by a high voltage ultra short pulsed X-ray source[4]. Weber *et al.* took streak photographs of the so-called "beam hole X-rays" which was caused by the interaction between the electron beam and the metal. They proposed the periodical closure-fallback mechanism for the formation of spiking[5].

In the previous report[2], the authors examined the method in which the edge welding phenomena was filmed by a high speed movie camera through a heat-proof glass, and also examined the method in which the image of the beam hole X-rays was visualized by a pin-hole camera and a X-ray image converter, and then it was also filmed by a high speed movie camera. In this report, in order to reveal the suppression mechanism of defects by the Tandem Electron Beam Welding Method, the images of beam hole X-rays were analysed by both a high speed

† Received on April 7, 1980

* Professor
** Research Instructor
*** Graduate Student, Osaka University

Transactions of JWRI is published by Welding Research Institute of Osaka University, Suita, Osaka, Japan

movie camera method mentioned above and a streak photograph method.

### 2-2 Experimental apparatus for observation of beam hole X-ray images

#### 2-2-1 High speed movie camera method

Figure 1 shows the layout of the filming apparatus. The image of beam hole X-rays, which is emitted from the

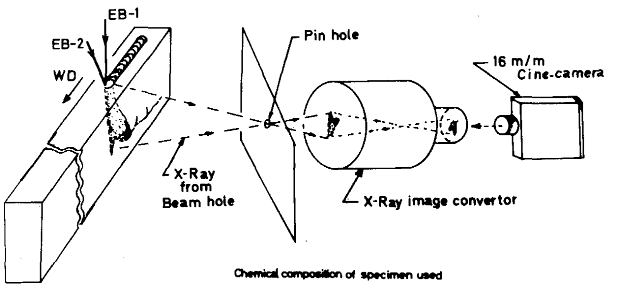


Chemical composition of specimen used

| element / material | Al | Cu | Si | Fe | Mn | Mg | Zn | Cr | Ti |
|---|---|---|---|---|---|---|---|---|---|
| Al 7075 | Bal | 2.3 | 0.13 | 0.35 | 0.10 | 3.6 | 7.0 | 0.19 | 0.04 |

wt(%)

**Fig. 1.** : Layout of filming apparatus.

interacting region of the electron beam with the metal, is focused on the input panel of a X-ray image converter, and then it is converted to a visible image on the output panel. Then it is filmed by a 16 mm high speed movie camera. The pin-hole is made from a lead sheet. The thickness of the sheet depends on the X-ray intensity, that is, accelerating voltage and current of the electron beam. In this experiment, the lead plate of 1 mm-thickness is used for accelerating voltage of 58 kV and current of 100 mA. On the other hand, the diameter of the pin-hole depends on the sensitivity and resolution of the X-ray image converter. Since the brightness of the output panel of the converter is finite, there is minimum X-ray intensity for maximum brightness. Therefore, the diameter of the pin-hole is decided to be 0.6 mm$\phi$ in this experiment in order to satisfy above minimum X-ray intensity and to make the size of the half-shadow smaller than that of the spatial resolution of the converter itself.

The images for various shutter speed are shown in photo 1. It is seen that since the shape of the image

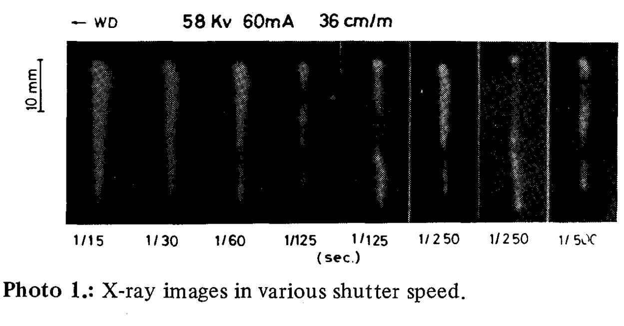


**Photo 1.:** X-ray images in various shutter speed.

changes with time very fast, it becomes wide with decreasing shutter speed. The time resolution depends on both the maximum brightness of the converter and the sensitivity of the movie film. In this experiment, the maximum time resolution is obtained in the condition that the shutter speed is 1/375 sec., the frame rate is 150 fps and the film of the sensitivity of ASA 400 is developed with 4 times higher sensitivity than that of standard.

#### 2-2-2 Streak photograph method

Figure 2 shows the explanation drowing for a streak photograph method. If the image of the output panel of the converter moves from up to down and the film moves from left to right at the same time, the image on the film becomes the line inclined to the left. In photo 2, an example of the streak photograph is shown. In this experiment, the moving speed of the film is the constant value of 23 cm/sec..

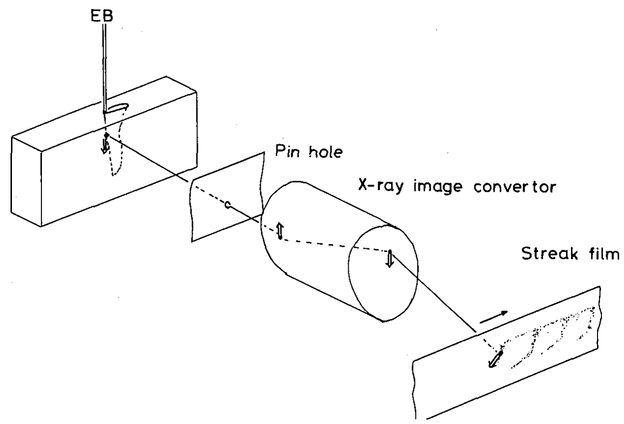


**Fig. 2.** : Explanation scheme for a streak photograph method.

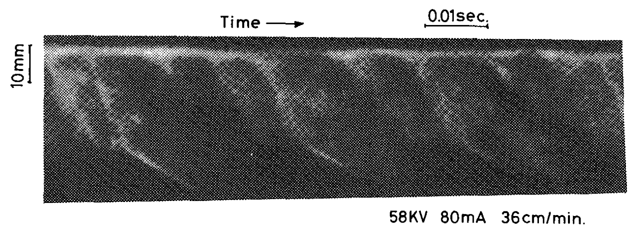


**Photo 2.:** An example of a streak photograph.

## 3. Analysis of the Formation Mechanism of Spiking

### 3-1 Analysis of the single electron beam welding

At first, these observation methods were applied to the analysis of the single electron beam welding. Photo 3 shows high speed photographs during the electron beam welding with the high power density beam. It is clearly

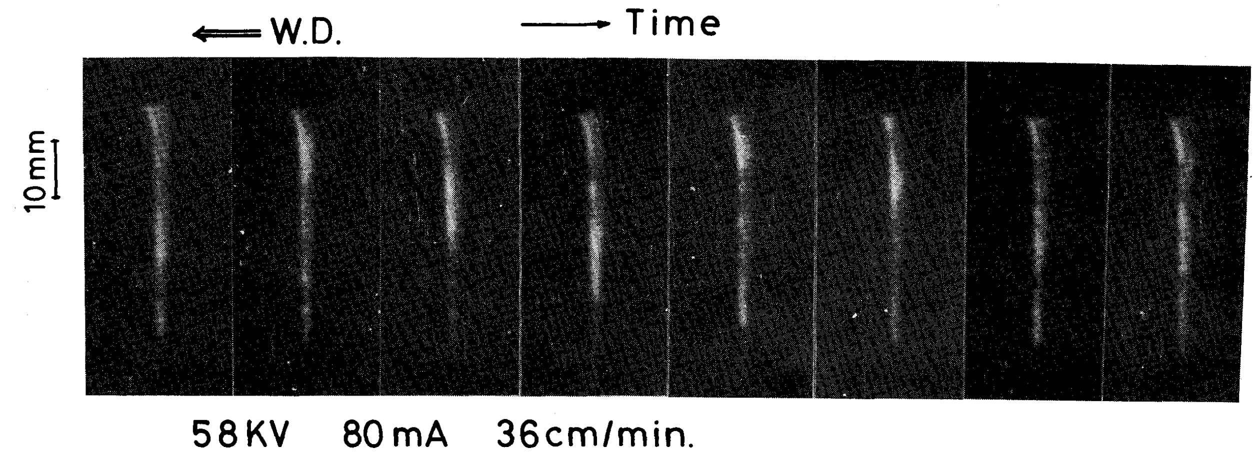


**Photo 3.:** Photographs in a high speed movie during electron beam welding with high power density beam.

seen that the image is not always stable but is changing with time. Because the electron beam reaches to the bright part, this means that the beam reaching depth is changing with time. It should be noticed that the bright point in the image seems to be moving downward. Furthermore, observing the images more carefully, it is found that the image is not simply perpendicular but it inclines with some degree against the normal direction.

From these facts, it is thought that the electron beam impinges to the front wall of the beam hole as illustrated in Fig. 3. The beam reaching depth ($h_b$), the angle of the front wall of the beam hole ($\theta$) are analysed for various power density or welding speed.

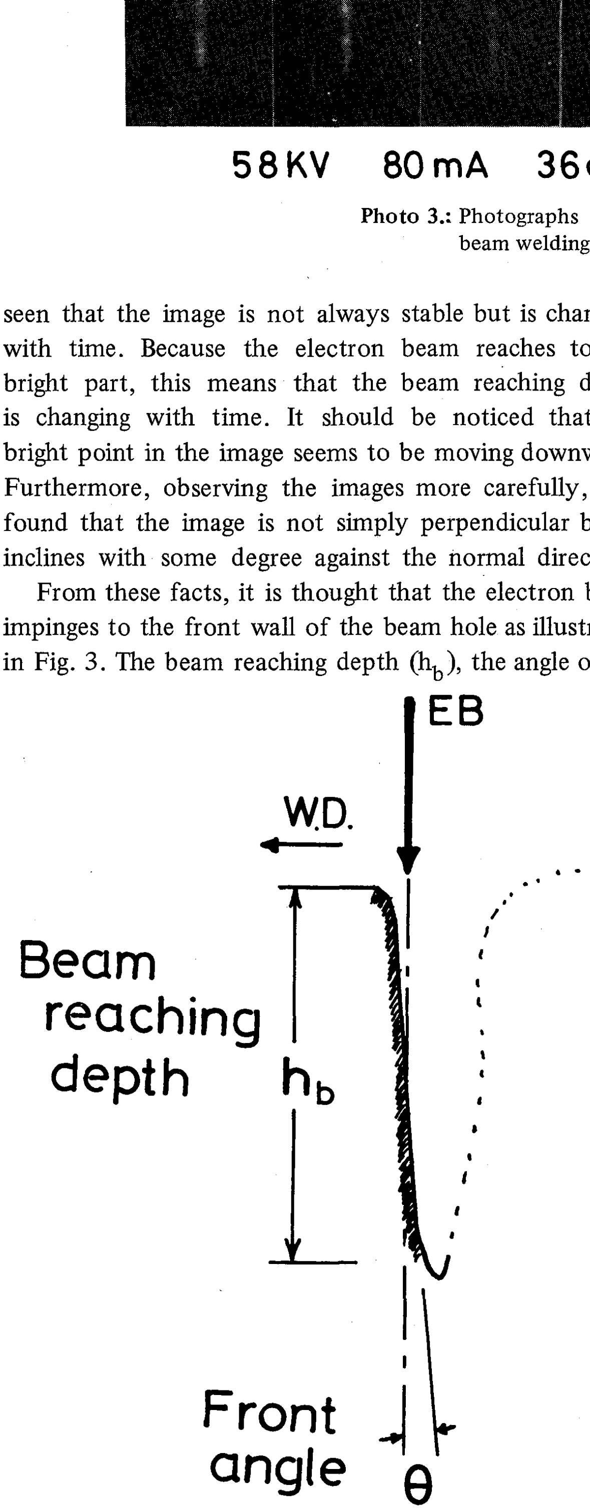


**Fig. 3.** : Beam reaching depth and front angle of beam hole.

### 3-1-1 Beam power density

Figure 4 shows the result of film analysis for $h_b$ and $\theta$ in case of high power density (Photo 3). Upper part of

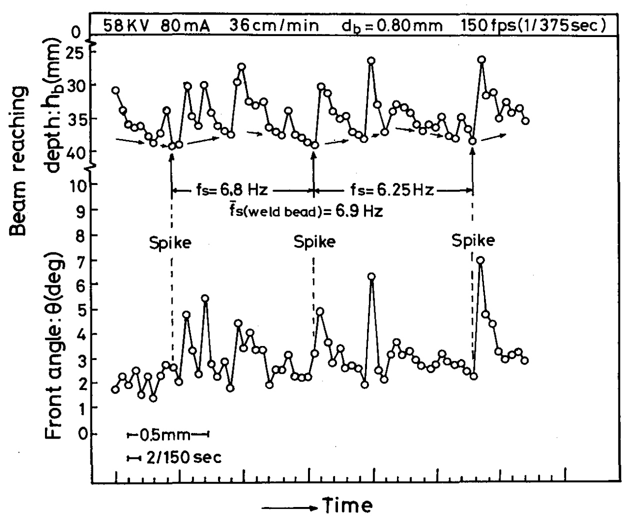


**Fig. 4.** : Film analysis for $h_b$ and $\theta$ in case of high power density shown in Photo 3. $f_s$ and $\bar{f}_s$ are spiking frequency in film analysis and in bead analysis, respectively.

this figure represents the change of the beam reaching depth and lower part the front angle. It is seen that both of them change periodically and the changes of these two parameters correspond each other. In other words, just after the beam reaching depth becomes large, the front angle becomes large. These facts mean that the electron beam does not always uniformly interact with the metal but there is a strongly interacting region (such a region is recorded on the film as a bright point) which melts the front wall of the beam hole locally. Therefore, the front wall is scraped not uniformly in time in case of high energy density beam. Film analyses in case of low energy density beam are shown in Fig. 5. Figures 4 and 5 are summarized to Fig. 6. It is seen that when the beam power density is small, the maximum beam reaching depth of cource decreases, while the fluctuations of the beam reaching depth and the mean front angle become also small. This change on fluctuation of the beam reaching depth corresponds with the occurance of the defects as shown in the longitudinal sections of the bead of Photo 4. Spiking phenomena grows up with increasing beam power density.

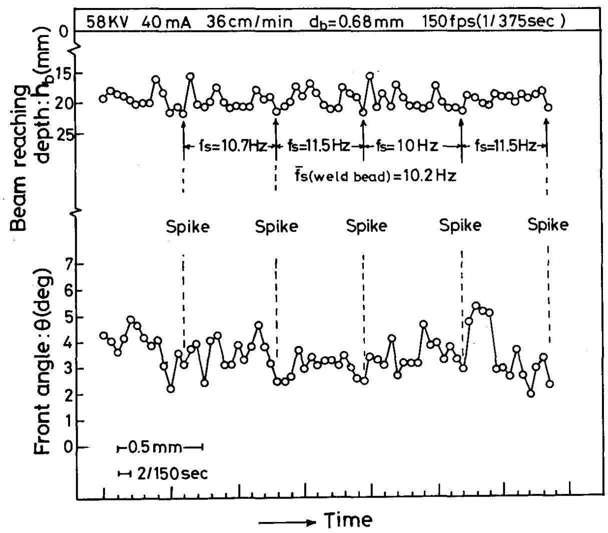


(a)

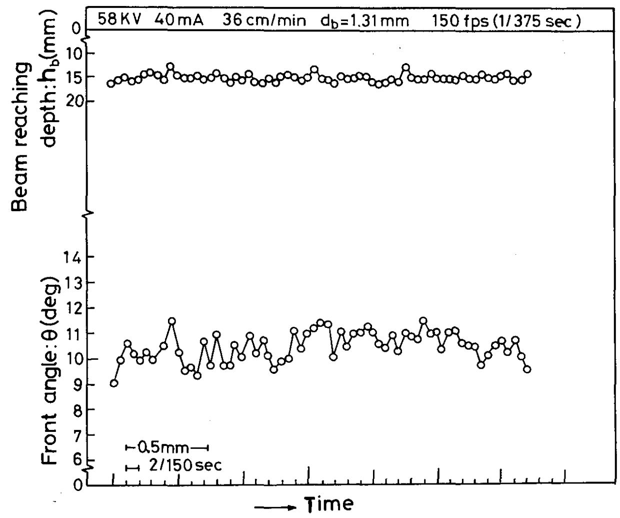


(b)

**Fig. 5(a) and (b).:** Film analysis for $h_b$ and $\theta$ in case of (a) middle power density and (b) low power density.

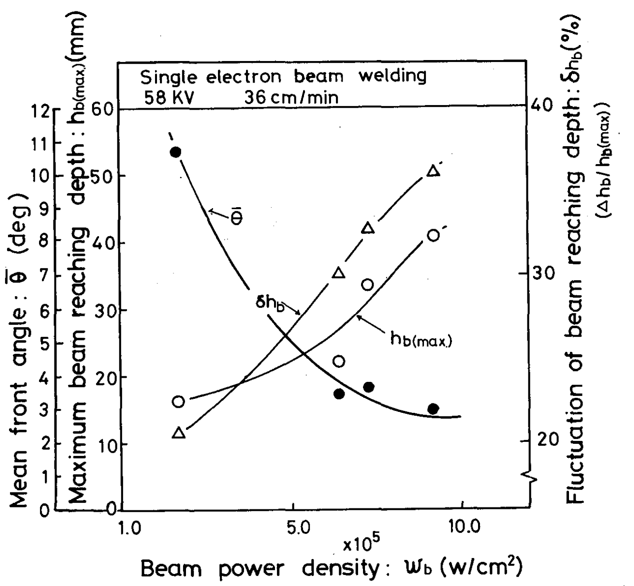


**Fig. 6.** : Dependency of $h_b$, $\delta h_b$ (its fluctuation) and $\bar{\theta}$ to power density.

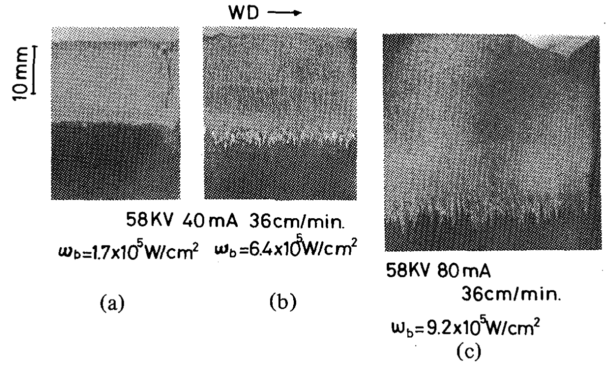


**Photo 4(a), (b) and (c).:** Londitudinal section of bead for various power density. (a): low, (b): middle and (c): high

### 3-1-2 Welding speed

Figure 7 shows the results of the film analyses in case of various welding speed. These figures are summalized in Fig. 8. As the welding speed becomes greater, the maximum beam reaching depth, the fluctuation of the beam reaching depth and the front angle also become smaller.

## 3-2 Formation process of spiking

These two results are summalized together as shown in Fig. 9 which represents the value of the beam reaching depth divided by the beam diameter and the front angle for various beam power density and welding speed. It is seen that the plots shift to the left corner with both increasing power density and decreasing welding speed. This means that the front wall becomes deep and steep. It is

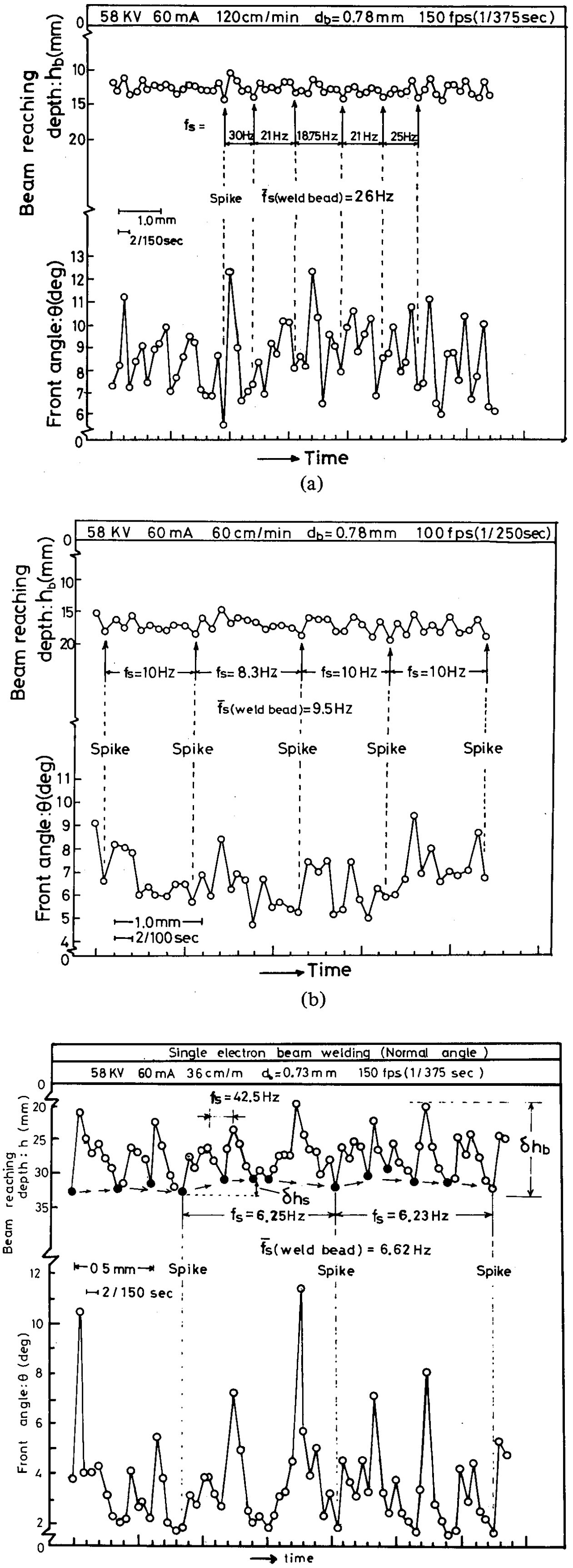


Fig. 7(a), (b) and (c).: Film analysis for $h_b$ and $\theta$ in various welding speed. (a): high, (b): middle and (c): low.

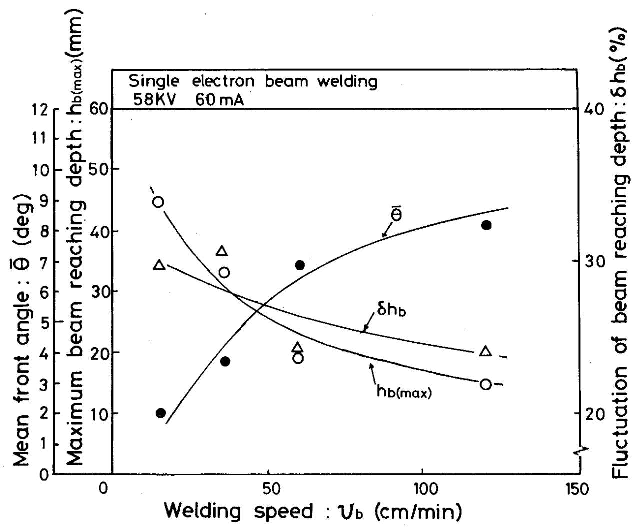


Fig. 8. : Dependency of $h_b$, $\delta h_b$ and $\bar{\theta}$ to welding speed.

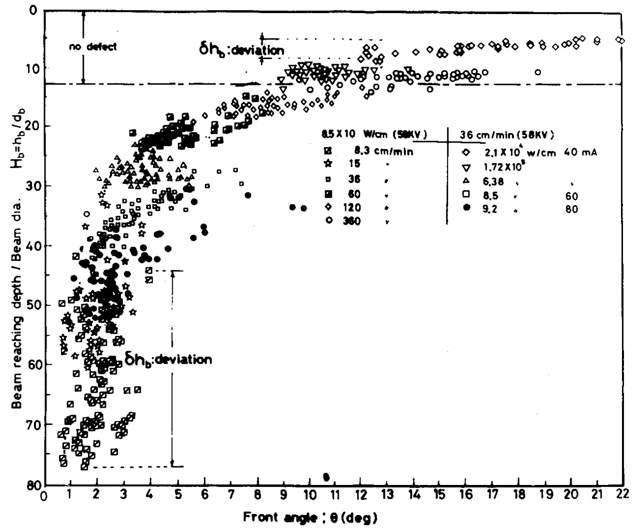


Fig. 9. : Dependency of $h_b$ and $\theta$ to both power density and welding speed.

also seen that the fluctuation in same specimen becomes large with increasing power density and decreasing welding speed. These facts mean that the beam power density or the welding speed, in other words, the heat input which is impinged into the specimen per unit area and unit time plays an important role for the formation of the beam hole, whose change affects the beam reaching depth and the front angle with their fluctuations. That is, as the heat input to the specimen per unit area and time increases, the electron beam reaching depth becomes large, and the front angle becomes small. This causes the increase of their fluctuations and unstability of the beam hole.

Summalizing these facts together, following model will be proposed for the welding process of the metal by the electron beam welding. The local region where the electron beam interacts the metal strongly occurs on the edge of the beam hole. Since the angle to the normal direction of this region is greater than other part on the front wall, the heat input on this region per unit area and time becomes greater than other parts. Therefore, this region melts down the front wall to the root of the beam hole. As this region come close to the root of the beam hole, the angle of the front wall becomes smaller. Then a steep front wall is formed. During this process, the electron beam goes ahead. Then such a region mentioned above (called the "shoulder") occures again near the top of the beam hole, which begins to scrape the front wall again. It will be thought that with repeating this process, the front wall of the beam hole goes ahead. This process is illustrated in Fig. 10. If this process is supposed, when the beam power density is very high, the beam reaching depth is very large and the angle of the front wall becomes very small. Then, the shoulder mentioned above impinges to the root of the beam hole strongly. In such case, the beam hole becomes deeper than usual and the spiking phenomena are brought about.

Streak photographs prove this model more directly.

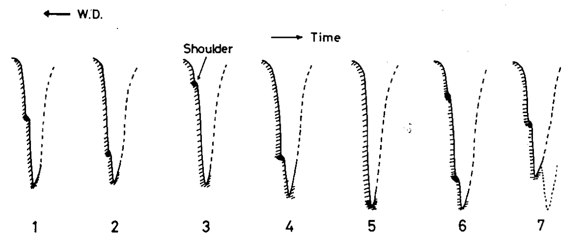


**Fig. 10.:** Scraping model for electron beam welding.

Photo 5(a) shows the streak photograph in case of high power density shown in Fig. 4. Discrete slant lines are clearly seen. If the interaction between the beam and the metal is uniform, the streak photograph should be seen as broad bright band shown in Photo 5(b). This fact indicates that the region where the electron beam interacts is a small region. Furthermore, the slope of these lines is classifyed into two kinds. This fact proves the stay of the shoulder at the root of the beam hole. In this second region where the beam stays, uneven penetration is brought about.

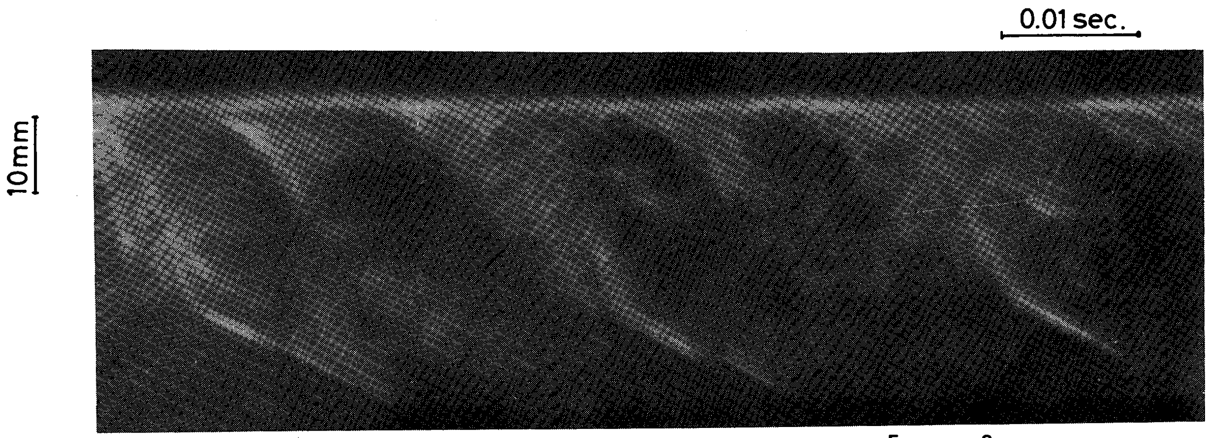


58 KV 80 mA 36 cm/min. $\omega_b = 9.2 \times 10^5 W/cm^2$

(a)

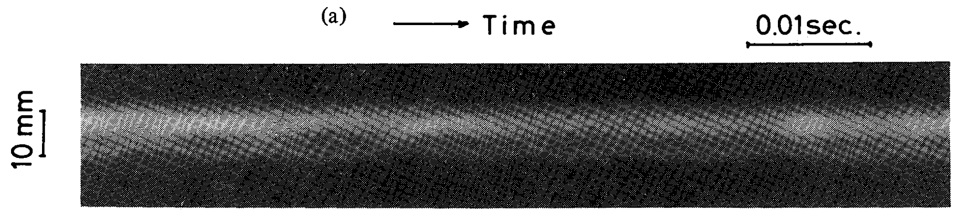


58 KV 40 mA 36 cm/min. $\omega_b = 0.2 \times 10^5 W/cm^2$

(b)

**Photo 5(a) and (b).:** Streak photographs for various power density. (a): high and (b):low.

## 4. Analysis of Suppression Mechanism of Defects

### 4-1 Tandem Electron Beam Welding

Photo 6 shows one frame of a high speed movie film of the image of beam hole X-rays during the Tandem Electron Beam Welding. The parameters of two electron

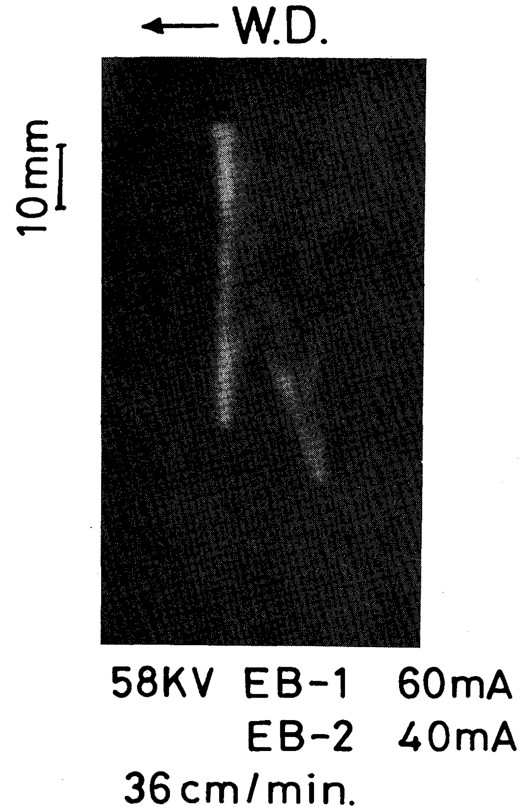


**Photo 6.:** Photograph in a high speed movie film of the Tandem Electron Beam Welding. Beam parameters are in the region of suppression of defects.

beams are in the region previously reported[2] where defects are suppressed successfully. It is proved that the second electron beam penetrates slightly deeper than the first beam. The film analysis for these two beams are shown in Fig. 11. The change for the first beam is quite the same tendency as the single electron beam which brings about the defects. However, for the second beam, the change of the beam reaching depth and front angle are small. From these facts, in the Tandem Electron Beam Welding, the following mechanism will be thought. The first beam plays the role of only deep penetration by a high power density and the second beam plays the role of only effective suppression of defects by a low power density. In this succeeded case, because the second electron beam is impinged into the beam hole made by the first beam and the rear wall of the beam hole is preheated by the first beam, the second beam, in spite of the low power density, penetrates easily into the metal. It is found that in the Tandem Electron Beam Welding, each beam displays fully their ability of deep penetration and repairment of defects.

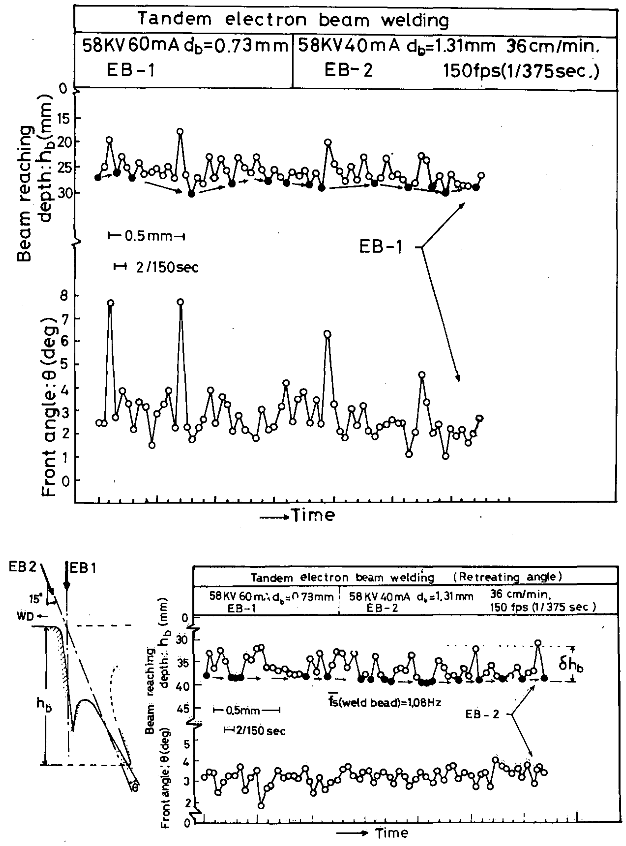


**Fig. 11.:** Film analysis for $h_b$ and $\theta$ in the Tandem Electron Beam Welding.

### 4-2 Single electron beam welding - beam oscillation method

The beam oscillation method has been used to suppress the defects in the single electron beam welding. However, there is a few research for its suppression mechanism. Therefore, the beam hole X-ray image during beam oscillation was analysed to compare with the Tandem Electron Beam Welding. It is well known that the direction of oscillation depends on the material and that the transverse oscillation is very effective for aluminum alloy. Therefore, the behaviour of the image of beam hole X-rays in the transverse oscillation was observed.

Figure 12 (a) shows the result of the film analysis for beam oscillation. It is seen that two parameters which were previously unstable become quite stable. Figures 12 (b) and (c) show the results of the film analyses in case of the different frequency. It is seen that the effect of beam oscillation dose not appear when the frequency is small. The results of the film analyses in case of various

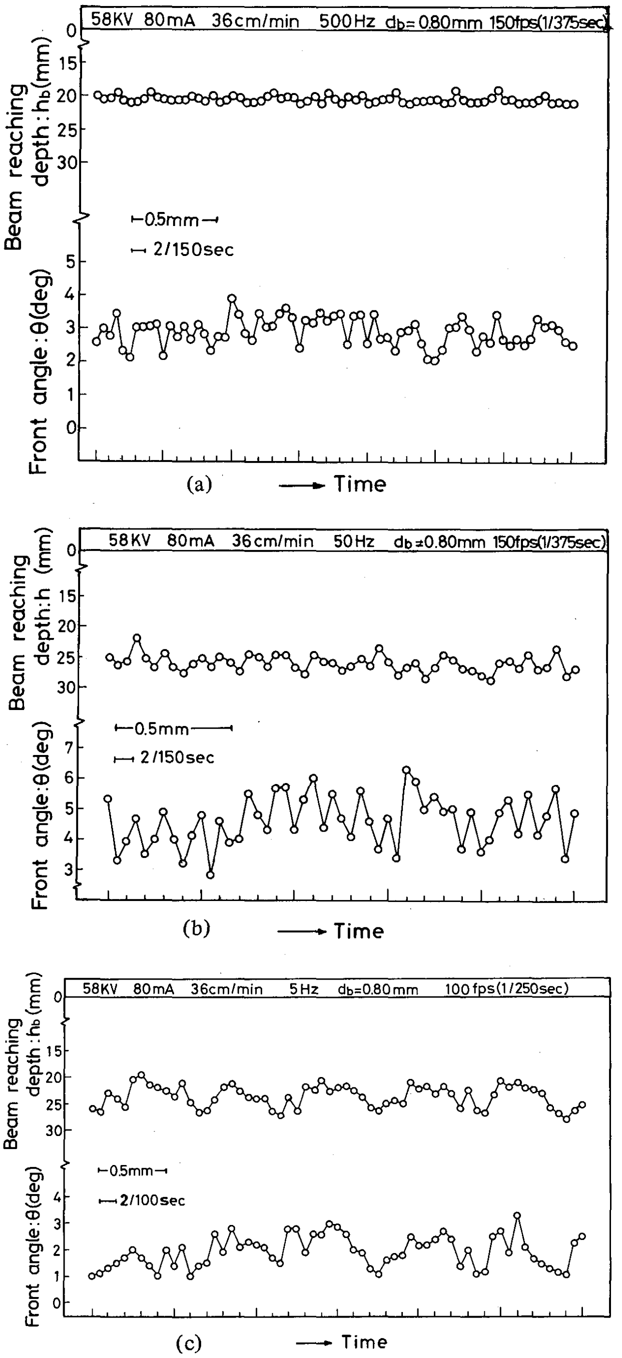


**Fig. 12(a), (b) and (c).:** Film analyses for $h_b$ and $\theta$ in beam beam oscillation of various frequency. (a): high, (b): middle and (c): low.

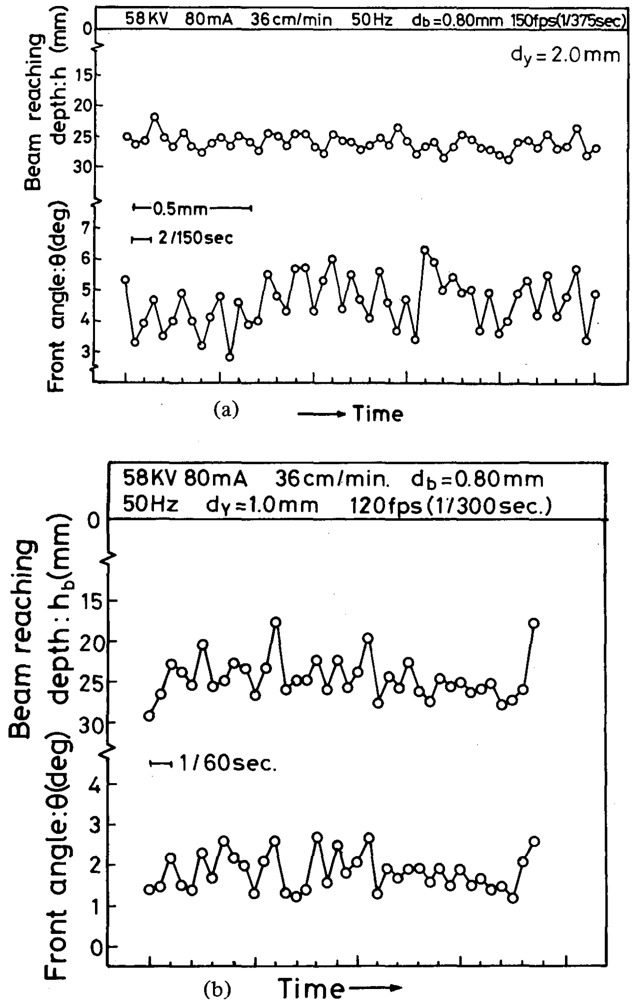


**Fig. 13(a) and (b).:** Film analyses for $h_b$ and $\theta$ in beam oscillation of various amplitude. (a): 2.0 mm and (b): 1.0 mm.

amplitude are shown in Fig. 13. It is seen that the effect of amplitude also appears from large frequency.

By using the streak photograph and the section of beads, these situation will be understood more clearly. In case of low frequency, very clear lines are seen in streak photograph (Photo 7 (a)), and both longitudinal and cross sections of bead indicate clearly that there are two kinds of beam hole (Photo 7 (b)). That is, the beam behaves as a

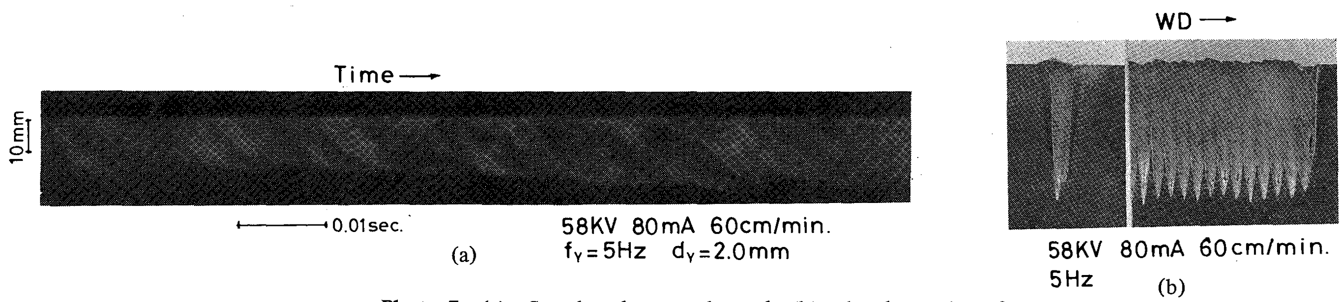


**Photo 7.: (a):** Streak photograph and (b): bead section for frequency of 5 Hz.

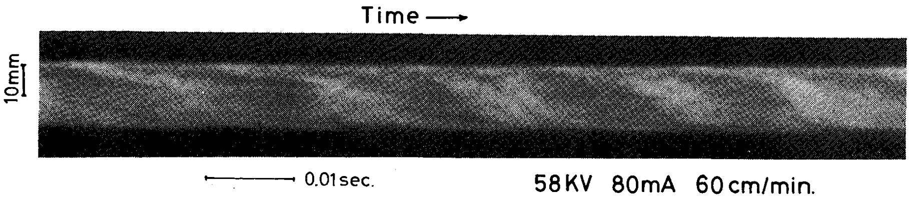


(a)

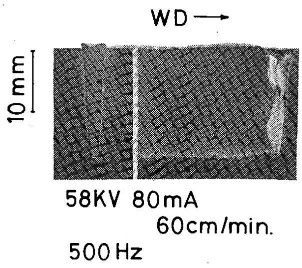


(b)

**Photo 8.: (a):** Streak photograph and (b): bead section for frequency of 500 Hz.

single electron beam moving diagonally. In case of high frequency, streak photograph seems to be rather uniform (Photo 8 (a)), and both loditudinal and cross sections of bead seems rather sound (Photo 8 (b)). This reason is thought that before the shoulder mentioned above reaches near the root, the electron beam is shifted by the beam oscillation of high frequency with interacting with the front wall uniformly.

### 4-3 Comparison of the Tandem Electron Beam and the single electron beam

When the suppression mechanism of the Tandem Electron Beam Welding compared with the single electron beam welding, the difference is clear. In case of the beam oscillation method, scraping characteristic of the beam itself is changed, because the beam is shifted before the shoulder reaches to the root. On the contrary, in case of the Tandem Electron Beam Welding, scraping characteristic is not changed. Therefore, in case of the beam oscillation method, much power is required for the same penetration depth. In case of the Tandem Electron Beam Welding, each beam displays their ability fully (the first beam is used only for the deep penetration and the second beam is used only for the repairement).

## 5. Conclusion

By using the pin-hole camera method with a X-ray image converter and a high speed movie camera, the image of beam hole X-rays emitted from the interacting region of the electron beam with the metal during welding is observed with time. It is also analysed with streak photographs and the section of the bead. From these analyses, following facts are found. The electron beam dose not always interact with the metal uniformly. There is the region where the electron beam interacts with the metal locally. It quickly melts the front wall downward periodically. It will thought that the spiking phenomena which appear frequently in a deep penetration welding occurs when the electron beam reaches the deeper part and the angle of the front wall of the beam hole becomes small, that is, when the region where the beam interacts strongly ("shoulder") reaches to the root of the beam hole. In the previous paper[2], it has already shown that the Tandem Electron Beam Welding Method can suppress such defects. In this report, the reason why it can suppress the defects is revealed. It is found that the defects made by the first beam are repaired by the second beam with reheating and remelting. In spite of the low power density than the first beam, the second beam easily penetrates deeper than the first beam, because the second beam is impinged into the beam hole made by the first beam and the root of the beam hole is preheated by the first beam.

By using the same method, suppression mechanism of defects by the beam oscillation method is also analysed. The beam seems to be changed in its characteristic from a single beam to a widened beam with increasing the frequency and amplitude. Finally it becomes the same as low power density beam.

It is thought that the beam oscillation makes the discrete scraping process of the shoulder mentioned above uniform. Therefore, in order to utilize that method effectively, it must be required that the scraping characteristic is in the region between a single beam and a widened beam. The comparison between the Tandem Electron Beam Welding Method and the beam oscillation method are performed. It is suggested that the former is better than the latter for the deep penetration welding, because the latter is decreased in its ability of penetration for improvement of the scraping characteristic, while the former is not changed in ability of each beam.

## References

1) : Y. Arata and E. Nabegata: Tandem Electron Beam Welding (Report I): Trans. JWRI, Vol. 7 (1978), No. 1, pp. 101-109.
2) : Y. Arata, E. Nabegata and N. Iwamoto: Tandem Electron Beam Welding (Report II): Trans. JWRI, Vol. 7 (1978), No. 2, pp. 233-243.
3) : H. Tong and W. H. Giedt: Radiographs of the Electron Beam Welding Cavity: Rev. Sci. Instrum., Vol. 40 (1969), No. 10, pp. 1283-1285.
4) : L.E. Bryant: Flash Radiography of Electron Beam Welding: Materials Evaluation, Vol. 29 (1971), No. 10, pp. 237-240.
5) : C. M. Weber, E. R. Funk and R. C. McMaster: Penetration Mechanism of Partial Penetration Electron Beam Welding: W. J., Vol. 51 (1972), No. 2, pp. 90s-94s.